Samiei et al., *BioImpacts,* 2022, 12(x), x-x
doi: 10.34172/bi.2022.23904
http://bi.tbzmed.ac.ir/

Injectable thermosensitive chitosan/gelatin hydrogel for dental pulp stem cells proliferation and differentiation

Mohammad Samiei[1,2], Elaheh Dalir Abdollahinia[1], Nazanin Amiryaghoubi[1], Marziyeh Fathi[1*], Jaleh Barar[1,3], Yadollah Omidi[4*]

[1]Research Center for Pharmaceutical Nanotechnology, Biomedicine Institute, Tabriz University of Medical Sciences, Tabriz, Iran
[2]Department of Endodontics, Faculty of Dentistry, Tabriz University of Medical Sciences, Tabriz, Iran
[3]Department of Pharmaceutics, Faculty of Pharmacy, Tabriz University of Medical Sciences, Tabriz, Iran
[4]Department of Pharmaceutical Sciences, College of Pharmacy, Nova Southeastern University, Fort Lauderdale, FL 33328, USA

Article Info

Article Type:
Original Article

Article History:
Received: 21 June 2021
Revised: 14 June 2022
Accepted: 15 June 2022
ePublished: 20 June 2022

Keywords:
Injectable hydrogel
Chitosan
Gelatin
Dental stem cells
Regenerative medicine
Tissue engineering

Abstract

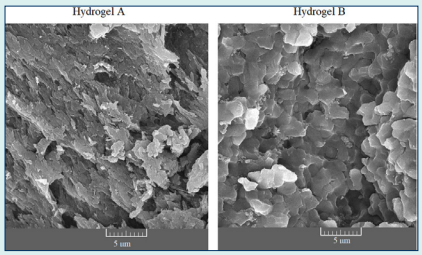

Introduction: Biocompatible and biodegradable scaffolds based on natural polymers such as gelatin and chitosan (CS) provide suitable microenvironments in dental tissue engineering. In the present study, we report on the synthesis of injectable thermosensitive hydrogel (PNIPAAm-g-CS copolymer/gelatin hybrid hydrogel) for osteogenic differentiation of human dental pulp stem cells (hDPSCs).

Methods: The CS-g-PNIPAAm was synthesized using the reaction of carboxyl terminated PNIPAAm with CS, which was then mixed with various amounts of gelatin solution in the presence of genipin as a chemical crosslinker to gain a homogenous solution. The chemical composition and microstructures of the fabricated hydrogels were confirmed by FT-IR and SEM analysis, respectively. To evaluate the mechanical properties (e.g., storage and loss modulus of the gels), the rheological analysis was considered. Calcium deposition and ALP activity of DPSCs were carried out using alizarin red staining and ALP test. While the live/dead assay was performed to study its toxicity, the real-time PCR was conducted to investigate the osteogenic differentiation of hDPSCs cultured on prepared hydrogels.

Results: The hydrogels with higher gelatin incorporation showed a slightly looser network compared to the other ones. The hydrogel with less gelatin indicates a rather higher value of G', indicating a higher elasticity due to more crosslinking reaction of amine groups of CS via a covalent bond with genipin. All the hydrogels contained viable cells with negligible dead cells, indicating the high biocompatibility of the prepared hydrogels for hDPSCs. The quantitative results of alizarin red staining displayed a significant rise in calcium deposition in hDPSCs cultured on prepared hydrogels after 21 days. Further, hDPSCs cultured on hydrogel with more gelatin displayed the most ALP activity. The expression of late osteogenic genes such as OCN and BMP-2 were respectively 6 and 4 times higher on the hydrogel with more gelatin than the control group after 21 days.

Conclusion: The prepared PNIPAAm-g-CS copolymer/gelatin hybrid hydrogel presented great features (e.g., porous structure, suitable rheological behavior, and improved cell viability), and resulted in osteogenic differentiation necessary for dental tissue engineering.

Introduction

Tooth damage can induce numerous difficulties such as problems in chewing and digestion of foods. It is caused by trauma, dental caries, tumor, and periodontal illnesses.[1-3] Tissue engineering is a multidisciplinary approach, which seems to revolutionize the regeneration of damaged tissues such as defects in dental tissue.[4] Tooth engineering is an encouraging novel therapeutic method that can favor substituting/regeneration of the lost tooth with a bioengineered technique or renovate the injured dental tissue. Dental tissue engineering consists of cells, scaffolds, and growth factors. The chief part of this method is the stem cells that are cultured on the surface of scaffolds, to generate a platform for stem cell proliferation, differentiation, and attachment.[5] Hydrogels have been chosen for numerous usages in tissue engineering, in large

*Corresponding authors: Marziyeh Fathi, Email: fathi.marziyeh@yahoo.com; Yadollah Omidi, Email: yomidi@nova.edu

part because of their exceptional biocompatibility, pliable techniques of synthesis, the array of several components, and appropriate physical properties.[6,7] Injectable hydrogels are a novel style of hydrogel network with definite fluidity that can be injected with a slightly invasive method into the damaged part like dental tissue.[8,9] Thermosensitive injectable hydrogels remain as a liquid at 25℃ and convert to gels after the injection into the body.[10] These types of hydrogels undergo reversible sol-gel transitions in physiological conditions with similar mechanical strength to those of alive organs.[11] Poly(*N*-isopropylacrylamide) (PNIPAAm) has been used to serve as one of the most widely thermo-sensitive polymers. PNIPAAm-based hydrogels provide a phase conversion in an aqueous solution and reveal a lower critical solution temperature (LCST) at nearby 33℃.[12-14] At temperatures below the LCST, a PNIPAAm-based hydrogel is extremely soluble in water due to the hydrogen interaction of amide groups with water molecules. Above the LCST, a PNIPAAm-based hydrogel is insoluble in an aqueous solution because the hydrogen interaction is weakened and the hydrophobic bonds between the methyl groups of ($-CH(CH_3)_2$) raise to be robust and so the hydrogels experience sudden and extreme shrinkage.[14,15] Chitosan (CS) is a hydrophilic and polycationic polymer attained by deacetylation of chitin with biocompatible, biodegradable, and non-toxic property, and wound-healing activity.[16] Most of these weird behaviors are related to the existence of main amines alongside the CS backbone.[17] CS has been widely utilized in dental tissue engineering usages.[18] For example, it is confirmed that hydrogels containing CS are extensively prepared for dental-pulp restoration because they can increase the growth, attachment, and odontoblastic differentiation of dental pulp stem cells (DPSCs) and mesenchymal stem cells (MSCs).[19,20] It was proven that sodium hyaluronate/CS polyelectrolyte scaffolds were biocompatible and nontoxic and enhanced the dental pulp regeneration.[21] In a study, a composite of CS/gelatin (Gel)/nanohydroxyapatite (CS/Gel/nHA) was fabricated for odontogenic differentiation of DPSCs. The results indicated the prepared scaffold enhanced the growth and biomineralization of DPSCs. Besides, the functional expressions of dentin sialophosphoprotein (DSPP), bone morphogenic protein-2 (BMP-2), and alkaline phosphatase activity (ALP) genes of DPSCs cultured on fabricated composite were upregulated that confirmed the formation of mineralized constructs on (CS/Gel/nHA) scaffold.[22] Gelatin is a protein product derived from collagen (Col) and is one of the most frequently utilized biomaterials for providing cellular platforms due to its biocompatible properties.[23] Lately, CS–Gel scaffolds have obtained much attention in numerous tissue regeneration applications due to their chemical resemblances to the extracellular matrix (ECM) in the natural organs, nontoxicity, and biodegradability.[24,25] It was proven that nano-fibrous Gel/silica bioactive glass (NF-Gel/SBG) promoted hDPSCs growth, odontogenic differentiation, and ALP activity and could be a suitable candidate for dentin/pulp tissue engineering.[26] In other work, three-dimensional-printed alginate-Gel hydrogel scaffolds enhanced odontoblastic differentiation of hDPSCs. Besides, the ALP activity and mineral deposition were promoted by the fabricated scaffold.[27] Genipin, a crystalline, water-soluble, natural, and non-toxic chemical crosslinking, is obtained from gardenia fruits.[28] It was proven that genipin-treated Col enhanced odontogenic differentiation and growth of hDPSCs. The odontogenic differentiation of hDPSCs was elevated by genipin via the extracellular signal-regulated kinase (ERK) signaling pathway. The ALP activity and mineral deposition were enhanced. The surface roughness and compressive properties of Col were increased by treatment with genipin.[29] In this work, a new design of hydrogel has been proposed as a carrier for hDPSCs benefiting from the desired properties of CS, PNIPAAm, and Gel. To this end, acid terminated PNIPAAm was synthesized and grafted to CS (PNIPAAm-g-CS) via amid condensation reaction. Subsequently, PNIPAAm-g-CS copolymer/Gel hybrid hydrogels were prepared with different ratios of Gel using genipin as a chemical crosslinker. The suitability of the prepared hydrogel for hDPSCs proliferation and differentiation was evaluated in vitro.

Materials and Methods

Materials

Medium molecular weight CS (degree of deacetylation= 75–85%), 1-ethyl-3-(3-dimethylaminopropyl) carbodiimide (EDC), N-hydroxysuccinimide (NHS), 2, 2'-azobis (isobutyronitrile) (AIBN), N-isopropylacrylamide (NIPAAm, 99%), genipin, p-nitrophenyl phosphate, 3-(4,5-dimethylthiazol-2-yl)-2,5-diphenyltetrazolium bromide (MTT), and alizarin red powder were supplied by Sigma-Aldrich (St. Louis, Missouri United States). 3-Mercaptopropionic acid (MPA), isopropyl alcohol, and gelatin were purchased from Merck. Dulbecco's modified eagle's medium F-12 (F-12 DMEM), fetal bovine serum (FBS), and antibiotics (Penicillin, Streptomycin), and all cell culture components were purchased from Invitrogen (Karlsruhe, Germany).

Synthesis of acid terminated PNIPAAm

Acid end-capped PNIPAAm was produced through free radical polymerization according to the reported procedure.[30] Briefly, NIPAAm (1 g), MPA (150 µL), and AIBN (20 mg) were dissolved in 20 mL of isopropanol and stirred under N_2 inert atmosphere for 30 minutes. Then, polymerization was carried out at 75°C for 12 hours under an N_2 atmosphere. After polymerization, the synthetic polymer was precipitated with an extra volume of cold diethyl ether. The precipitated polymer was dried under vacuum and subsequently, dissolved in deionized water and dialyzed against deionized water for 3 days to

remove unreacted monomers and chemicals. Ultimately, the refined PNIPAAm-COOH was lyophilized and stored.

Synthesis of CS-g-PNIPAAm

The CS-g-PNIPAAm was synthesized by the reaction of carboxyl terminated PNIPAAm with CS in the presence of NHS and EDC.[30] For this purpose, CS (60 mg) was dissolved in 1% acetic acid under continuous stirring at room temperature, and then, PNIPAAm-COOH (200 mg) was mixed with this solution. Afterward, the EDC/NHS with weight ratios of 1:2 (450 mg/900 mg) was added to the mixture, and the reaction was continued for 12 hours at 25°C. The product solution was dialyzed against distilled water for 2 days to eliminate unreacted reagents and then lyophilized for future usage.

Synthesis of the thermosensitive injectable hydrogels of CS-g-PNIPAAm using gelatin and chemical crosslinker

CS-g-PNIPAAm (80 mg) was dissolved in 2 mL (hydrogel A) or 3 mL (hydrogel B) of gelatin solution (2 % (w/v)) and mixed for a while to gain a homogenous solution. Then genipin (2 mg) and $NaHCO_3$ (10 mg) were added to the solution to distribute uniformly in each sample and were mixed for 30 minutes at room temperature. Then, the solution was kept at 37°C to form the gel in an incubator to attain dark blue color. The gelation time of hydrogels was determined by applying the test tube inverting method. The fabricated hydrogels were frozen at -70°C and lyophilized for further characterizations.

Structural characterization of the prepared hydrogels

Structural characterization of the synthesized PNIPAAm-COOH, CS-g-PNIPAAm, and hydrogels was carried out by FT-IR Tensor 27 spectrometer (Bruker Optik GmbH, Ettlingen,

Germany) in the range of 4000 to 400 cm^{-1} using KBr powder. Scanning electron microscopy (SEM) was applied to evaluate the structure and morphology of the prepared hydrogels by TESCANMIRA3 electron microscope (FE-SEM, MIRA3 FEG-SEM Tescan, Czech). For the SEM analysis, freeze-dried samples were first coated with a gold layer. The storage (G′) and loss modulus (G″) of the prepared hydrogels were measured with the frequency dependence in the range from 0.1 to 10 Hz via a parallel plate rheometer (Anton Paar, MCR-301, Austria). The samples were placed between parallel plates (25 mm in diameter) with a gap distance of 400 µm and conductions were performed at 37°C at 0.2 % strain and angular frequency of 1 rad s^{-1}.

Human dental pulp stem cells (DPSCs) culture and in vitro cellular evaluations

Human dental pulp stem cells (hDPSCs) from the Iranian Biological Resource Center were grown at a contained seeding density in Dulbecco's-modified Eagle's media (DMEM-F12; Inoclon, Tehran, IRAN). Media consisted of 20% fetal bovine serum (FBS; Gibco, NY, USA) and 2 mM L-Glutamine (Inoclon, Tehran, IRAN) at 37°C and 5% CO_2. Cells were collected and subcultured using 0.25% trypsin until they achieved 80% confluence (Inoclon, Tehran, IRAN). The culture media was changed every two days, and hDPSCs from the third and sixth passages were included in the subsequent experiments. Three groups, including control, hydrogel A, and hydrogel B were evaluated for cell growth in two different media (normal medium (NM)/differentiation medium (DM)). The DM as an osteogenic medium included 50 µg/mL of ascorbic acid (AA), 10 mM of β-GP, and 10 nM of dexamethasone.

Live/dead assay

To investigate the effect of the hydrogel matrix on hDPSCs proliferation, the survival of cultured hDPSCs was assessed on different hydrogels and the control group using a live/dead kit. To prepare the sterile hydrogels, autoclaved CS powder was dissolved in sterile hydrochloric acid (0.1 M) solution and the β-GP solution was sterilized using a 0.22 µm syringe and subsequently, hydrogels were prepared as described above. Hydrogels' solution was added to 24-well culture plates (0.25 mL/well) and incubated at 37°C for gel formation. Then, hDPSCs at a seeding density of 5.0×10^4 cells/well were cultured on the gel surface and incubated for 7 days. To prepare the staining solution, 1 µL of Calcein-AM stock solution (4 mM Calcein-AM stock solution in dimethyl sulfoxide (DMSO)) and 1 µL of ethidium homodimer-1 (EthD-1) stock solution (2 mM EthD-1 stock in diluted DMSO/H_2O) were added in 2 mL PBS under no-light conditions. After 7 days, the staining solution was added to the samples cultured in a 24-cell plate with a cell density of 5×10^4. Then, the stained plate was wrapped in aluminum foil and placed in the incubator for 45 minutes. Images of stained samples were prepared using Cytation™ 5 imaging reader at wavelengths of 420 and 480 nm. Viable cells in different groups were indicated by the observation of calcein-AM or the lack of EthD-1 signal, while the existence of EthD-1 signal detected dead cells.

Alizarin red staining (ARS) analyses

Calcium secretion of cultured hDPSCs on hydrogels was detected in the differentiation medium using ARS analysis. Hydrogels were prepared and distributed in 24-well culture plates (250 µL per well). After gel-forming, hDPSCs with a cell density of 2.5×10^4 were cultured on each well for 21 days. Each group received a fresh osteogenic medium every three days. After 3 weeks of cell culture, the cells were washed twice with PBS and fixed with 4% formaldehyde for 20 minutes. Then, the cells were washed with an appropriate amount of deionized water (×3) for 10 minutes. Finally, the samples were stained with 40 mM/L ARS for 15 minutes to analyze the calcium deposits of hDPSCs. The stained samples were washed with deionized water (×5) to remove the extra stains, and

the cells were imaged using an inverted microscope. To measure the quantity of ARS, 200 µL of 10% acetic acid (v/v) (AcOH) was applied to each well of a 24-well plate to extract bound AR into the solution and incubated at room temperature for 30 minutes. Then, pipette cutting head tips were used to gather the cells, which were moved to a 1.5 mL microcentrifuge tube containing 10% AcOH. After 30 seconds of rotating, the samples were incubated on ice for 5 minutes before being exposed at 85°C for 10 minutes. After centrifuging the samples at 10,000g for 20 minutes, 200 µL of the supernatant was moved to a new tube. To neutralize the acids, 75 µL of 10% (v/v) ammonium hydroxide was applied to the samples. Each sample's absorbance at 405 nm was measured using an ELISA spectrophotometer. The standard AR curve was used to calculate the calcium content in each well.

ALP assay

ALP activity was assessed after 21 days in cultured hDPSCs (initial seeding cell density 2.5×10^4) under a differentiation medium. Briefly, the wells were washed with PBS (3×). Then, 400 µL of cell digestion buffer (including the buffer storage solution (1.5 M Tris -HCl, 1 mM $ZnCl_2$, $MgCl_2$ $6H_2O$) was diluted in dH_2O (1:10), and 1% Triton X-100) was applied to each well. The cells were then incubated for 30 minutes at 37°C before being deposited overnight at 4°C. After that, cell lysates were transferred into the tubes, vortexed for 2 minutes, and centrifuged at 2000 rpm for 5 minutes. On a 96-well plate, approximately 10 µL of each cell lysate was mixed with 190 µL of ALP solution (37.1 mg pNPP in 20 mL cellular buffer). The Cytation 5™ system was used to measure ALP activity absorption at 405 nm.

RNA extraction, cDNA synthesis, and qPCR

On day 21, the expression of osteogenic genes was examined in the samples mentioned above with an initial cell density of 2.5×10^4. Total RNA was collected from each sample using the standard TRIzol procedure and solubilized in 20 µL of RNase-free water. RNA concentration was determined using the NanoDrop 2000 spectrophotometer at 260 nm (NanoDrop Technologies, Wilmington, DE, USA). The cDNA was reverse-transcripted according to the manufacturer's instructions through a Thermo Fisher scientific kit. In this step, 1 µg of each isolated RNA was mixed with 1 µL of Random Hexamer and a certain proportion of DNase-RNase free water to make a total volume of 12 µL for each PCR reaction. They were heated to 65°C for 5 minutes before being placed on ice for 10 minutes. For each sample, the main mixture was formed by adding 4 µL RT buffer (5x), 1 µL dNTP (200 U/µL), 1 µL MLV (200 U/µL), 1 µL RNase inhibitor (100 uU/µL), and 1 µL free-RNAase water. PCR reaction in one-step PCR (SimpliAmp) was performed by applying 8 µL of the main mixture to PCR tubes at 25°C for 10 minutes, 43°C for 1 hour, 70°C for 10 minutes, and 8°C for 5 minutes. The RT-PCR green SYBR protocol and the iQ5-BioRad RT-PCR approach were used to confirm osteogenic gene expression in hDPSCs (Bio-Rad; Hercules, CA, USA). In brief, the RT-PCR reaction mixture included 1 µL of cDNA, 8 µL of DNase-RNase free water, 0.5 µL of reverse primer, 0.5 µL of the forward primer, and 10 µL of SYBR Green PCR (2x) (Dajon, Korea: BIO FACT Co., Ltd.). RT-PCR was performed following temperature cycling conditions. Amplification was done with initial activation phase for 10 minutes at 94°C followed by 40 cycles of denaturation phase for 15 seconds at 94°C, different annealing temperatures (Table 1) for 30 seconds, lasting 30 seconds at 72°C, and final extension for 10 minutes at 72°C. The Pfaffl approach was used to examine the relative fold variations in the expression pattern.[31]

Statistical analysis

ANOVA was used for statistical analysis, followed by a multiple comparison post hoc test. The mean values and standard deviations (SD) were used to represent data. Statistical significance was defined as a *P* value less than 0.05. GraphPad Prism software version 6.0 was utilized for statistical analysis.

Results and Discussion

Hydrogel preparation and characterization

The synthesis and preparation steps of the hydrogels are shown in Fig. 1. In this study, to achieve the

Table 1. Primer sequences used in the analysis of RT-PCR

Gene name	Abbreviation	Forward/Reverse primers (5'→3')	Annealing temperature (°C)
Alkaline phosphatase	ALP	AAACTGGGGCCTGAGATACC GCACTCAAGCCAATGGTCTG	58
Bone Morphogenetic Protein 2	BMP-2	GTGCTTCTTAGACGGACTG GAACTCGCTCAGGACCTCG	52.2
Osteocalcin	OCN	CAGCGAGGTAGTGAAGAGAC GCCAACTCGTCACAGTCC	60.5
Runx Family Transcription Factor 2	Runx2	CAGACCAGCAGCAGCACTCCATA CAGCGTCAACACCATCATTC	59
Glyceraldehyde 3-phosphate dehydrogenase	GAPDH	CCTGCTTCACCACCTTCTTG CCATCACCATCTTCCAGGAG	58.5

thermosensitive and biocompatible hydrogel, in the first step acid terminated PNIPAAm was prepared and used for the grafting with amine functional groups of CS. Finally, to benefit from the advantages of gelatin, the hydrogel of CS-g-PNIPAAm incorporated with gelatin was conducted using genipin as a chemical crosslinker. The sol-gel transition was investigated with an inverted tube test at 37°C that indicated a fast gelation time of around 1 minute.

Fig. 2 indicates the FT-IR spectra of PNIPAAm-COOH, CS-g-PNIPAAm, and the synthesized hydrogels. The characteristic peaks at 1649, 1545, and 1461 cm^{-1} are contributed to amide I, amide II, and C-N bands of PNIPAAm-COOH. In the FT-IR spectrum of CS-g-PNIPAAm, amide bands of CS and PNIPAAm overlapped, while bands corresponding to the methyl groups of PNIPAAm at 1385 cm^{-1} and C-O of CS around 1096 cm^{-1} were observed that could demonstrate the grafting of PNIPAAm to CS.[30,32] In the FT-IR spectra of prepared hydrogels A and B, characteristic peaks of CS-g-PNIPAAm were shifted somehow; while due to the similarity of gelatin functional group, there were no new peaks by introducing the gelatin moiety.

Microstructures of the prepared hydrogels were confirmed by SEM images (Fig. 3). A high porous network structure is obvious for the prepared hydrogel samples confirming the high water permeability to the amorphous parts of hydrogels that provide a suitable environment for cell adhesion and proliferation as well as drug loading

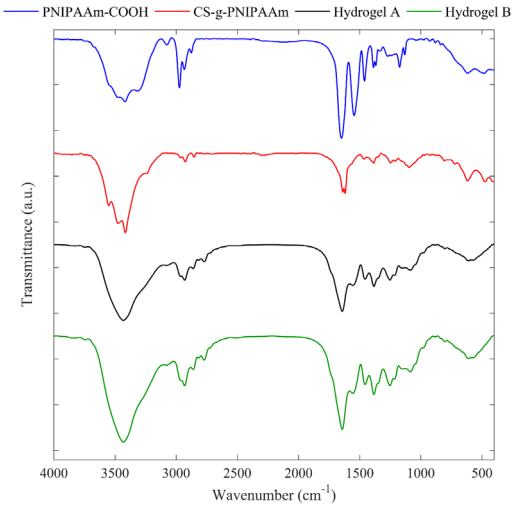

Fig. 2. The FT-IR spectra of PNIPAAm, CS-g-PNIPAAm, hydrogel A, and hydrogel B.

and release purposes.[33] Hydrogel B shows a slightly looser network compared to hydrogel A due to the higher gelatin incorporation.

To evaluate the mechanical properties of the gels, the rheological analysis with frequency sweeping can be considered where stronger hydrogel has a higher G' value (elastic response) compared to G" (viscose response) that confirms a "gel-like" phase.[34] Therefore, dynamic rheological analysis was done with frequency sweeping

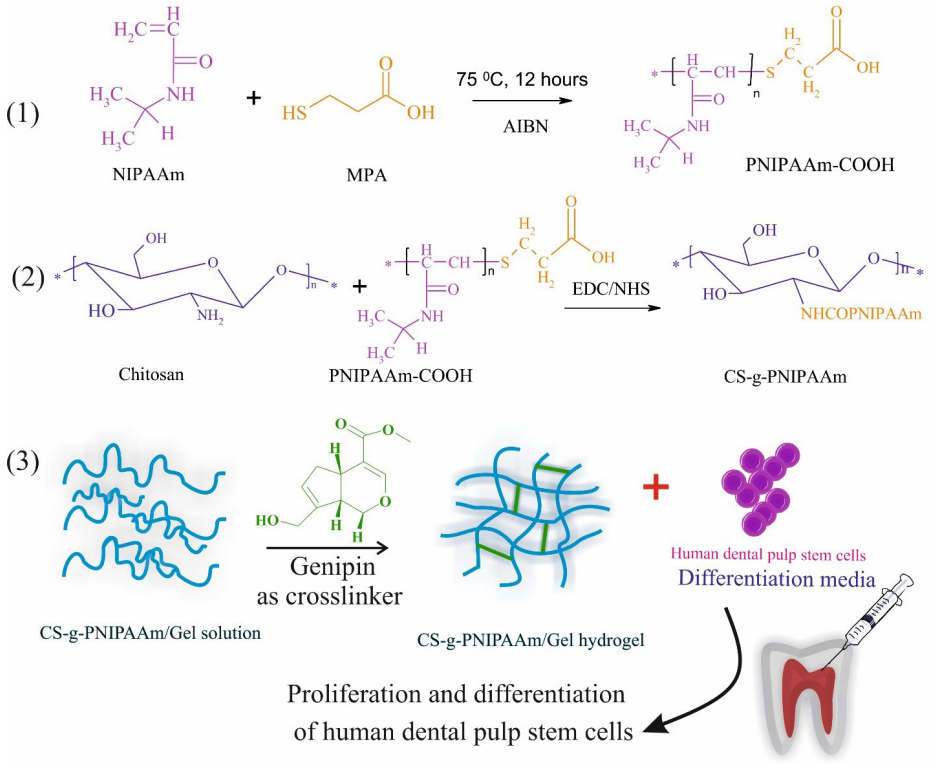

Fig. 1. Schematic presentation of hydrogel preparation steps and their biomedical application.

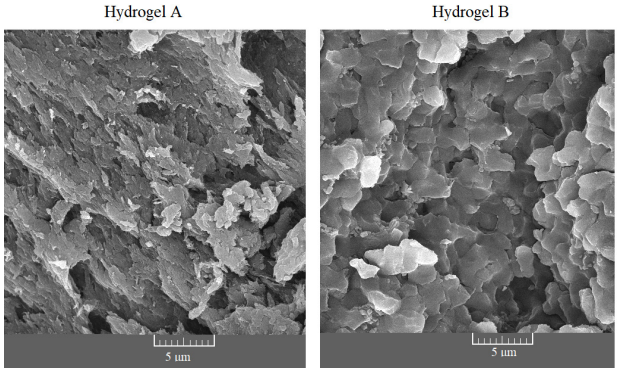

Fig. 3. The SEM micrographs of the hydrogels A and B. Different morphological features are seen between hydrogel A and hydrogel B.

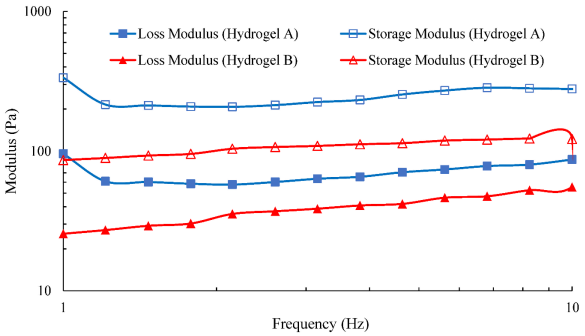

Fig. 4. The storage (G′) and loss (G″) modulus for hydrogels A and B at 37°C.

(Fig. 4). The G′ of both hydrogels are higher than G" and hydrogel A indicates a rather higher value of G' compared to hydrogel B indicating a higher elasticity. This can be attributed to the more crosslinking reaction of amine groups of CS via a covalent bond with genipin and reducing the chain mobility in hydrogel A.

Cell viability in synthesized hydrogels

In 2D and 3D cultures, the viability of 7-day-old cultured hDPSCs was evaluated with live-dead calcein-AM (green) and EthD-1 (red) staining (Fig. 5). The ratio of green to red fluorescence intensity showed the level of cell viability. The presence of the prepared hydrogels did not decrease cell viability, which was greatly enhanced, suggesting that the developed hydrogels have a beneficial effect on biological activity in vitro similar to cellular expansion and development within a hydrogel scaffold.[35] According to Fig. 4, all of the hydrogels contained viable cells with very few dead cells (red), indicating that the hDPSCs developed well on the hydrogel throughout the incubation period. As a result of the observed activity of PNIPAAm as a 3D scaffold during cell development, the soft matrix appears to retain optimal properties for long-term use in bone tissue engineering and tooth regeneration.[36] Besides, CS was applied to PNIPAAm to enhance cell attachment, reinforce mechanical properties, and facilitate cell proliferation.[37-39]

The ARS investigation of calcium deposition

ARS is an incredibly flexible tool for measuring calcium deposition because it is simple to obtain for quantification.[40] Calcium formation is critical in ECM mineralization. A red complex is formed when ARS interacts with calcium cations.[41-43] Fig. 6A shows that the osteogenic medium induced red color and dark spots in groups exposed to the differentiation medium.[44,5] The quantitative results indicate that a substantial rise in Ca deposition ($P < 0.05$) occurs in cell-cultured on hydrogel substrate at day 21 compared to the control groups (Fig. 6B).[46]

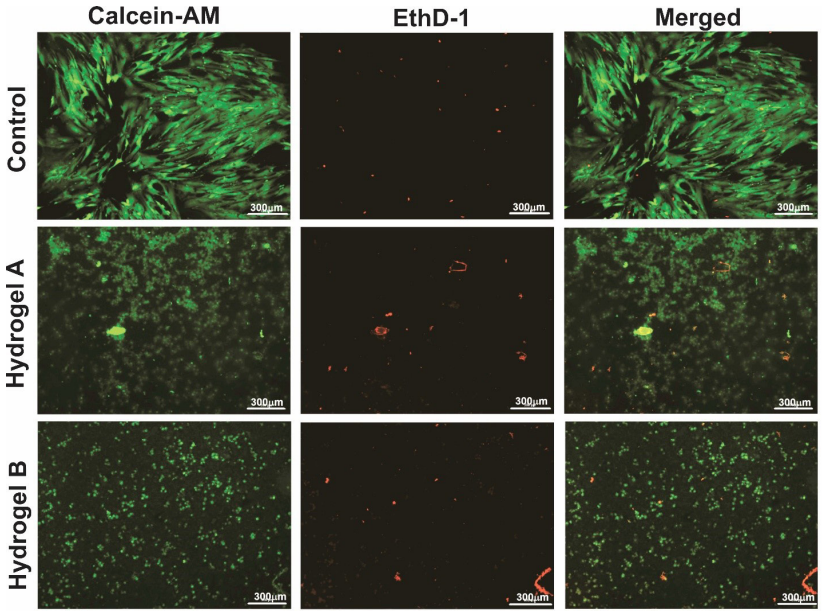

Fig. 5. The viability of hDPSCs using the live/dead kit cultured in different groups, including 2D culture, hydrogel A, and hydrogel B. The green and red hDPSCs were labeled using Calcein-AM and EthD-1, respectively. Scale bar: 300 μm.

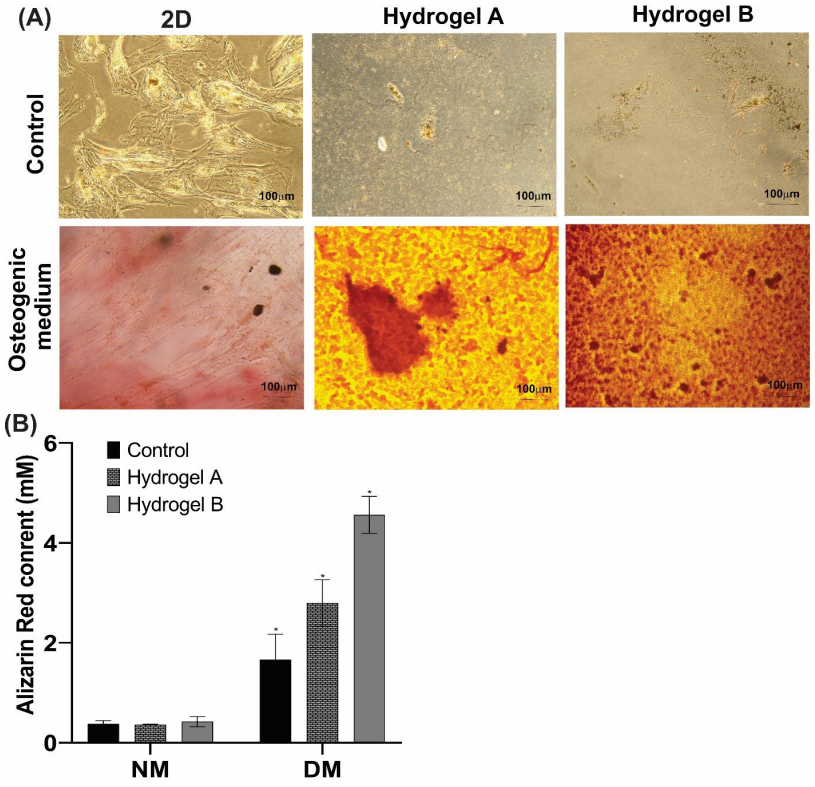

Fig. 6. The osteogenic behavior of the hDPSCs treated with the hydrogels A and B. (A) Alizarin red staining (ARS) microscopic images of the treated and untreated hDPSCs in both regular and differential media for 21 days. (B) The histogram of the calcium storage in the treated hDPSCs measured by ARS (absorbance at 405 nm). The ARS for each group was calculated using the standard curve (* P <0.05). Scale bar: 100 µm. NM: Normal medium; DM: Differentiation media.

ALP activity analysis in the synthesized hydrogel

ALP is one of the most critical osteogenic biomarkers in the early stages of mineralization. It belongs to the zinc metalloprotein enzyme family. ALP can promote phosphate aggregation for hydroxyapatite in ECM by catalyzing p-nitrophenyl phosphate (pNPP) hydrolysis and the removal of phosphate to inorganic phosphate and p-nitrophenol (pNP), which then improves mineral deposits by a collection of inorganic phosphates and Ca^{2+} as a result of mineralization.[47] The ALP enzyme promotes the differentiation of hDPSCs to an osteoblast phenotype and is recognized as an early osteogenic marker of bone differentiation. Fig. 7 shows that alkaline phosphatase expression was higher in the group cultured in the differential medium than the control group (P<0.05). hDPSCs cultured on hydrogel B had the most ALP activity. But there was no substantial difference in hydrogel groups in different mediums. Taken together, chitosan and PNIPAAm are suitable substrates for growth and cell proliferation, which increase ALP expression.[39, 48]

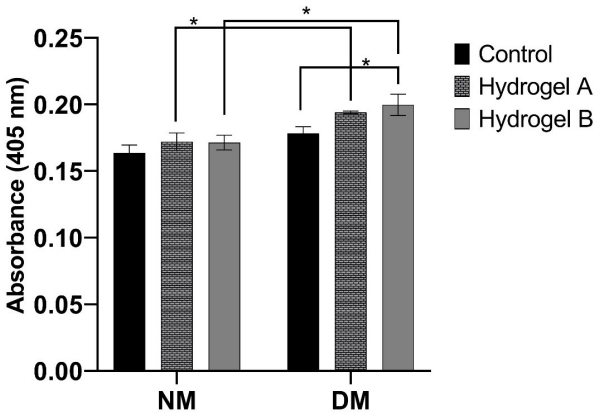

Fig. 7. The ALP activity of hDPSCs in (A) the control and (B) the osteogenic supplement media on day 21. The differences between the groups were measured and shown (* P <0.05). NM: Normal medium; DM: Differentiation medium.

Gene expression analysis in the synthesized hydrogel

As shown in Fig. 8, the expression of osteogenic genes was studied to determine the osteogenic differentiation of hDPSCs in hydrogels. There is a direct relationship between serum bone ALP quantities and bone development, with the majority of ALP activation and mineralization occurring during osteogenic initiation.[49,50] *Runx2*, a specific transcription factor, serves an essential function in osteogenic development. It can stimulate osteogenesis-related gene expression, control the progression of the cell cycle, and enhance a suitable microenvironment for osteogenesis. All these seem to favor a multitude of signaling pathways such as TGF, BMP, Notch, Wnt, Hedgehog, and FGF in the early stage of osteogenic induction.[51,52] In particular, BMP-2 is a well-known inductive growth

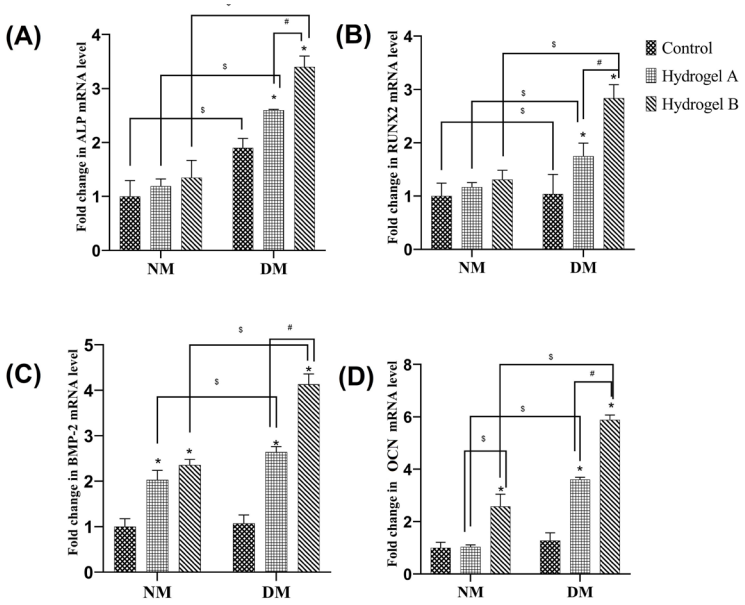

Fig. 8. The expression of osteogenic differentiation genes: (A): ALP; (B): Runx; (C): BMP, and (D) OCN normalized to the internal GAPDH gene. *, #, $ show statistically significant difference ($P < 0.05$) with the internal control, hydrogels, and corresponding groups in different media. NM: Normal medium; DM: Differentiation medium.

factor for osteogenic differentiation of various stem cells.[53,54] The OCN gene encodes a non-collagen protein that is only found in osteoblasts. In the structure of the OCN protein, glutamic acid has a high affinity for calcium ions (Ca^{2+}). Reducing OCN's proclivity for Ca^{2+} results in less osteogenic differentiation.[55-57] Greater concentrations of Ca^{2+} have been shown to influence bone development and stem cell differentiation.[58,59] In this analysis, there is a specific pattern of expressed osteogenic genes in most of the studied groups. The expression of osteogenic genes improved in differentiated conditions compared to normal conditions. According to this study, hDPSCs cultured on hydrogels in differentiated media have the highest osteogenic gene expression. Comparing corresponding groups in normal and differential culture media revealed that the differentiation medium promotes osteogenic gene expression more effectively ($P>0.05$). On day 21, the expression of osteogenic genes expressed at the late stage of osteoblast differentiation, such as OCN and BMP-2, was significant, approximately 6 and 4 times higher on the hydrogel B than in the control group, respectively ($P>0.05$). In hDPSCs cultured on hydrogel B in a differentiation medium, the expression of the osteogenic genes ALP and Runx, expressed in the early stages of osteoblast development, is 3 and 2 times in comparison to the control group, respectively. Because of the high percentage of gelatin, the ability of cell differentiation in hydrogel B is higher than that in other groups. The gelatin in the scaffold structure promotes cell attachment, biodegradability, and differentiation.[60]

Conclusion

To establish a safe and robust thermo-responsive hydrogel, PNIPAAm-g-CS copolymer/Gel hybrid hydrogels were prepared with different ratios of Gel using genipin as a chemical crosslinker for dental tissue engineering and were characterized by utilizing a variety of techniques. Based on our findings, the fabricated hydrogel seems to mimic the in vivo ECM feature providing a permissive microenvironment with high biocompatibility for the growth of hDPSCs. The prepared hydrogels promoted the expression of osteogenic genes such as BMP and OCN along with ALP activity and calcium formation. These results indicate that the synthesized scaffold can provide an osteogenic environment without the application of exogenous agents. Thus, the scaffold might be used for the osteogenic differentiation of hDPSCs in dental tissue engineering.

Acknowledgments

The authors would like to acknowledge the technical support of the Research Center for Pharmaceutical Nanotechnology.

Funding sources

This work was part of a Ph.D. thesis supported by the Research Center for Pharmaceutical Nanotechnology at Tabriz University of Medical Sciences (#59150).

Ethical statement

This study was approved by the Ethics Committee of Tabriz University of Medical Sciences, Tabriz, Iran (ID number: IR.TBZMED.VCR.REC.1398.122).

Competing interests

YO, JB, and MF act as editorial members of the journal. As part of the journal policy, the peer-review process was conducted by independent reviewers and editors based on the Editorial Policies and Publication Ethics of the journal (https://bi.tbzmed.ac.ir/EditorialPolicies). Other co-authors declare that there is no conflict of interests.

YO and MF conceptualized and designed the study. MS, EDA, and NAY

Research Highlights

What is the current knowledge?

√ Biocompatible and biodegradable scaffolds based on natural polymers such as chitosan and gelatin in combination with thermosensitive PNIPAAm can provide suitable microenvironments for dental tissue engineering.

√ The CS-g-PNIPAAm/gelatin hybrid hydrogels were fabricated and evaluated as a new scaffold for the proliferation and differentiation of hDPSCs.

What is new here?

√ The potential of the prepared hydrogels for dental tissue engineering was assessed by investigating the structural analysis, biocompatibility tests, and also expression of ALP, Runx, BMP, and OCN genes using real-time PCR for osteogenic differentiation of hDPSCs.

√ The results indicated that the developed hydrogels especially with a higher value of gelatin could be considered an attractive candidate for dental tissue engineering purposes.

performed the experiments, collected the data, analyzed the data, and wrote the manuscript. YO supervised the project. MF, JB, and YO edited and finalized the manuscript. All authors read and approved the final manuscript.

References

1. Dosumu O, Ogunrinde J, Bamigboye S. Knowledge of consequences of missing teeth in patients attending prosthetic clinic in UCH Ibadan. *Ann Ib Postgrad Med.* **2014**; 12: 42-8.
2. Li G, Zhou T, Lin S, Shi S, Lin Y. Nanomaterials for craniofacial and dental tissue engineering. *J Dent Res* **2017**; 96: 725-32. https://doi.org/10.1177/0022034517706678
3. Young C, Terada S, Vacanti J, Honda M, Bartlett J, Yelick P. Tissue engineering of complex tooth structures on biodegradable polymer scaffolds. *J Dent Res* **2002**; 81: 695-700. https://doi.org/10.1177/154405910208101008
4. Rosa V, Della Bona A, Cavalcanti BN, Nör JE. Tissue engineering: from research to dental clinics. *Dent Mater* **2012**; 28: 341-8. https://doi.org/10.1016/j.dental.2011.11.025
5. Lymperi S, Ligoudistianou C, Taraslia V, Kontakiotis E, Anastasiadou E. Dental stem cells and their applications in dental tissue engineering. *Open Dent J* **2013**; 7: 76. https://doi.org/10.2174/1874210601307010076
6. Buenger D, Topuz F, Groll J. Hydrogels in sensing applications. *Prog Polym Sci* **2012**; 37: 1678-719. https://doi.org/10.1016/j.progpolymsci.2012.09.001
7. Slaughter BV, Khurshid SS, Fisher OZ, Khademhosseini A, Peppas NA. Hydrogels in regenerative medicine. *Adv Mater* **2009**; 21: 3307-29. https://doi.org/10.1002/adma.200802106
8. Wu J, Chen Q, Deng C, Xu B, Zhang Z, Yang Y, *et al.* Exquisite design of injectable Hydrogels in Cartilage Repair. *Theranostics* **2020**; 10: 9843. https://doi.org/10.7150/thno.46450
9. Chang B, Ahuja N, Ma C, Liu X. Injectable scaffolds: Preparation and application in dental and craniofacial regeneration. *Mater Sci Eng R Rep* **2017**; 111: 1-26. https://doi.org/10.1016/j.mser.2016.11.001
10. Wang Q, Zuo Z, Cheung CKC, Leung SSY. Updates on thermosensitive hydrogel for nasal, ocular and cutaneous delivery. *Int J Pharm* **2019**; 559: 86-101. https://doi.org/10.1016/j.ijpharm.2019.01.030
11. Kim MS, Park SJ, Chun HJ, Kim C-H. Thermosensitive hydrogels for tissue engineering. *Tissue Eng Regen Med* **2011**; 8: 117-23.
12. Gil ES, Hudson SM. Stimuli-reponsive polymers and their bioconjugates. *Prog Polym Sci* **2004**; 29: 1173-222. https://doi.org/10.1016/j.progpolymsci.2004.08.003
13. Zhang X-Z, Xu X-D, Cheng S-X, Zhuo R-X. Strategies to improve the response rate of thermosensitive PNIPAAm hydrogels. *Soft Matter* **2008**; 4: 385-91. https://doi.org/10.1039/B713803M
14. Wei H, Cheng S-X, Zhang X-Z, Zhuo R-X. Thermo-sensitive polymeric micelles based on poly (N-isopropylacrylamide) as drug carriers. *Prog Polym Sci* **2009**; 34: 893-910. https://doi.org/10.1016/j.progpolymsci.2009.05.002
15. Jain K, Vedarajan R, Watanabe M, Ishikiriyama M, Matsumi N. Tunable LCST behavior of poly (N-isopropylacrylamide/ionic liquid) copolymers. *Polym Chem* **2015**; 6: 6819-25. https://doi.org/10.1039/C5PY00998G
16. Jayakumar R, Prabaharan M, Reis R, Mano J. Graft copolymerized chitosan—present status and applications. *Carbohydr Polym* **2005**; 62: 142-58. https://doi.org/10.1016/j.carbpol.2005.07.017
17. Croisier F, Jérôme C. Chitosan-based biomaterials for tissue engineering. *Eur Polym J* **2013**; 49: 780-92. https://doi.org/10.1016/j.eurpolymj.2012.12.009
18. Tang G, Tan Z, Zeng W, Wang X, Shi C, Liu Y, *et al.* Recent Advances of Chitosan-Based Injectable Hydrogels for Bone and Dental Tissue Regeneration. *Front Bioeng Biotechnol* **2020**; 8: 1084. https://doi.org/10.3389/fbioe.2020.587658
19. Ducret M, Montembault A, Josse J, Pasdeloup M, Celle A, Benchrih R, *et al.* Design and characterization of a chitosan-enriched fibrin hydrogel for human dental pulp regeneration. *Dent Mater* **2019**; 35: 523-33. https://doi.org/10.1016/j.dental.2019.01.018
20. Bordini EAF, Cassiano FB, Silva ISP, Usberti FR, Anovazzi G, Pacheco LE, *et al.* Synergistic potential of 1α, 25-dihydroxyvitamin D3 and calcium–aluminate–chitosan scaffolds with dental pulp cells. *Clin Oral Investig* **2020**; 24: 663-74. https://doi.org/10.1007/s00784-019-02906-z
21. Coimbra P, Alves P, Valente TAM, Santos R, Correia I, Ferreira P. Sodium hyaluronate/chitosan polyelectrolyte complex scaffolds for dental pulp regeneration: synthesis and characterization. *Int J Biol Macromol* **2011**; 49: 573-9. https://doi.org/10.1016/j.ijbiomac.2011.06.011
22. Vagropoulou G, Trentsiou M, Georgopoulou A, Papachristou E, Prymak O, Kritis A, *et al.* Hybrid chitosan/gelatin/nanohydroxyapatite scaffolds promote odontogenic differentiation of dental pulp stem cells and in vitro biomineralization. *Dent Mater* **2021**; 37: e23-e36. https://doi.org/10.1016/j.dental.2020.09.021
23. Yung C, Wu L, Tullman J, Payne G, Bentley W, Barbari T. Transglutaminase crosslinked gelatin as a tissue engineering scaffold. *J Biomed Mater Res A* **2007**; 83: 1039-46. https://doi.org/10.1002/jbm.a.31431
24. Huang Y, Onyeri S, Siewe M, Moshfeghian A, Madihally SV. In vitro characterization of chitosan–gelatin scaffolds for tissue engineering. *Biomaterials* **2005**; 26: 7616-27. https://doi.org/10.1016/j.biomaterials.2005.05.036
25. Afewerki S, Sheikhi A, Kannan S, Ahadian S, Khademhosseini A. Gelatin-polysaccharide composite scaffolds for 3D cell culture and tissue engineering: Towards natural therapeutics. *Bioeng Transl Med* **2019**; 4: 96-115. https://doi.org/10.1002/btm2.10124
26. Qu T, Liu X. Nano-structured gelatin/bioactive glass hybrid scaffolds for the enhancement of odontogenic differentiation of human dental pulp stem cells. *J Mater Chem B* **2013**; 1: 4764-72. https://doi.org/10.1039/C3TB21002B
27. Yu H, Zhang X, Song W, Pan T, Wang H, Ning T, *et al.* Effects of 3-dimensional bioprinting Alginate/Gelatin hydrogel scaffold extract on proliferation and differentiation of human dental pulp stem cells. *J Endod* **2019**; 45: 706-15. https://doi.org/10.1016/j.joen.2019.03.004
28. Muzzarelli RA. Genipin-crosslinked chitosan hydrogels as biomedical and pharmaceutical aids. *Carbohydr Polym* **2009**; 77: 1-9. https://doi.org/10.1016/j.carbpol.2009.01.016
29. Kwon Y-S, Lim E-S, Kim H-M, Hwang Y-C, Lee K-W, Min K-S. Genipin, a cross-linking agent, promotes odontogenic differentiation of human dental pulp cells. *J Endod* **2015**; 41: 501-7. https://doi.org/10.1016/j.joen.2014.12.002

30. Rejinold NS, Sreerekha P, Chennazhi K, Nair S, Jayakumar R. Biocompatible, biodegradable and thermo-sensitive chitosan-g-poly (N-isopropylacrylamide) nanocarrier for curcumin drug delivery. *Int J Biol Macromol* **2011**; 49: 161-72. https://doi.org/10.1016/j.ijbiomac.2011.04.008
31. Pfaffl MW. A new mathematical model for relative quantification in real-time RT–PCR. *Nucleic Acids Res* **2001**; 29: e45. https://doi.org/10.1093/nar/29.9.e45
32. Chen JP, Cheng TH. Thermo-responsive chitosan-graft-poly (N-isopropylacrylamide) injectable hydrogel for cultivation of chondrocytes and meniscus cells. *Macromol Biosci* **2006**; 6: 1026-39. https://doi.org/10.1002/mabi.200600142
33. Fathi M, Alami-Milani M, Geranmayeh MH, Barar J, Erfan-Niya H, Omidi Y. Dual thermo-and pH-sensitive injectable hydrogels of chitosan/(poly (N-isopropylacrylamide-co-itaconic acid)) for doxorubicin delivery in breast cancer. *Int J Biol Macromol* **2019**; 128: 957-64. https://doi.org/10.1016/j.ijbiomac.2019.01.122
34. Amiryaghoubi N, Pesyan NN, Fathi M, Omidi Y. Injectable thermosensitive hybrid hydrogel containing graphene oxide and chitosan as dental pulp stem cells scaffold for bone tissue engineering. *Int J Biol Macromol* **2020**; 162: 1338-57. https://doi.org/10.1016/j.ijbiomac.2020.06.138
35. Hendrick V, Muniz E, Geuskens G, Wérenne J. Adhesion, growth and detachment of cells on modified polystyrene surface. *Cytotechnology* **2001**; 36: 49-53. https://doi.org/10.1023/A:1014041003617
36. Rivero RE, Capella V, Liaudat AC, Bosch P, Barbero CA, Rodríguez N, *et al.* Mechanical and physicochemical behavior of a 3D hydrogel scaffold during cell growth and proliferation. *RSC Adv* **2020**; 10: 5827-37. https://doi.org/10.1039/C9RA08162C
37. Cho JH, Kim SH, Park KD, Jung MC, Yang WI, Han SW, *et al.* Chondrogenic differentiation of human mesenchymal stem cells using a thermosensitive poly(N-isopropylacrylamide) and water-soluble chitosan copolymer. *Biomaterials* **2004**; 25: 5743-51. https://doi.org/10.1016/j.biomaterials.2004.01.051
38. Ohya S, Kidoaki S, Matsuda T. Poly(N-isopropylacrylamide) (PNIPAM)-grafted gelatin hydrogel surfaces: interrelationship between microscopic structure and mechanical property of surface regions and cell adhesiveness. *Biomaterials* **2005**; 26: 3105-11. https://doi.org/10.1016/j.biomaterials.2004.08.006
39. Smith E, Yang J, McGann L, Sebald W, Uludag H. RGD-grafted thermoreversible polymers to facilitate attachment of BMP-2 responsive C2C12 cells. *Biomaterials* **2005**; 26: 7329-38. https://doi.org/10.1016/j.biomaterials.2005.05.060
40. Gregory CA, Gunn WG, Peister A, Prockop DJ. An Alizarin red-based assay of mineralization by adherent cells in culture: comparison with cetylpyridinium chloride extraction. *Anal Biochem* **2004**; 329: 77-84. https://doi.org/10.1016/j.ab.2004.02.002
41. Yang H, Zhao X, Xu Y, Wang L, He Q, Lundberg YW. Matrix recruitment and calcium sequestration for spatial specific otoconia development. *PLoS One* **2011**; 6: e20498. https://doi.org/10.1371/journal.pone.0020498
42. Wang X, Gu Z, Jiang B, Li L, Yu X. Surface modification of strontium-doped porous bioactive ceramic scaffolds via poly(DOPA) coating and immobilizing silk fibroin for excellent angiogenic and osteogenic properties. *Biomater Sci* **2016**; 4: 678-88. https://doi.org/10.1039/c5bm00482a
43. Lievremont M, Potus J, Guillou B. Use of alizarin red S for histochemical staining of Ca2+ in the mouse; some parameters of the chemical reaction in vitro. *Acta Anat (Basel)* **1982**; 114: 268-80. https://doi.org/10.1159/000145596
44. Jeon J, Lee MS, Yang HS. Differentiated osteoblasts derived decellularized extracellular matrix to promote osteogenic differentiation. *Biomaterials Research* **2018**; 22: 4. https://doi.org/10.1186/s40824-018-0115-0
45. Hanna H, Mir LM, Andre FM. In vitro osteoblastic differentiation of mesenchymal stem cells generates cell layers with distinct properties. *Stem Cell Res Ther* **2018**; 9: 203. https://doi.org/10.1186/s13287-018-0942-x
46. Liao HT, Chen CT, Chen JP. Osteogenic differentiation and ectopic bone formation of canine bone marrow-derived mesenchymal stem cells in injectable thermo-responsive polymer hydrogel. *Tissue Eng Part C Methods* **2011**; 17: 1139-49. https://doi.org/10.1089/ten.tec.2011.0140
47. Chang YL, Stanford CM, Keller JC. Calcium and phosphate supplementation promotes bone cell mineralization: implications for hydroxyapatite (HA)-enhanced bone formation. *J Biomed Mater Res* **2000**; 52: 270-8. https://doi.org/10.1002/1097-4636(200011)52:2<270::aid-jbm5>3.0.co;2-1
48. Amir LR, Suniarti DF, Utami S, Abbas B. Chitosan as a potential osteogenic factor compared with dexamethasone in cultured macaque dental pulp stromal cells. *Cell Tissue Res* **2014**; 358: 407-15. https://doi.org/10.1007/s00441-014-1938-1
49. Zajdel A, Kałucka M, Kokoszka-Mikołaj E, Wilczok A. Osteogenic differentiation of human mesenchymal stem cells from adipose tissue and Wharton's jelly of the umbilical cord. *Acta Biochim Pol* **2017**; 64: 365-9. https://doi.org/10.18388/abp.2016_1488
50. Castrén E, Sillat T, Oja S, Noro A, Laitinen A, Konttinen YT, *et al.* Osteogenic differentiation of mesenchymal stromal cells in two-dimensional and three-dimensional cultures without animal serum. *Stem Cell Res Ther* **2015**; 6: 167. https://doi.org/10.1186/s13287-015-0162-6
51. Xu J, Li Z, Hou Y, Fang W. Potential mechanisms underlying the Runx2 induced osteogenesis of bone marrow mesenchymal stem cells. *Am J Transl Res* **2015**; 7: 2527-35.
52. Loebel C, Czekanska EM, Bruderer M, Salzmann G, Alini M, Stoddart MJ. In vitro osteogenic potential of human mesenchymal stem cells is predicted by Runx2/Sox9 ratio. *Tissue Eng Part A* **2015**; 21: 115-23. https://doi.org/10.1089/ten.TEA.2014.0096
53. Bragdon B, Moseychuk O, Saldanha S, King D, Julian J, Nohe A. Bone morphogenetic proteins: a critical review. *Cell Signal* **2011**; 23: 609-20. https://doi.org/10.1016/j.cellsig.2010.10.003
54. Jung T, Lee JH, Park S, Kim YJ, Seo J, Shim HE, *et al.* Effect of BMP-2 Delivery Mode on Osteogenic Differentiation of Stem Cells. *Stem Cells Int* **2017**; 2017: 7859184. https://doi.org/10.1155/2017/7859184
55. Komori T. What is the function of osteocalcin? *J Oral Biosci* **2020**; 62: 223-7. https://doi.org/10.1016/j.job.2020.05.004
56. Hauschka PV, Lian JB, Cole DE, Gundberg CM. Osteocalcin and matrix Gla protein: vitamin K-dependent proteins in bone. *Physiol Rev* **1989**; 69: 990-1047. https://doi.org/10.1152/physrev.1989.69.3.990
57. Price PA, Otsuka AA, Poser JW, Kristaponis J, Raman N. Characterization of a gamma-carboxyglutamic acid-containing protein from bone. *Proc Natl Acad Sci U S A* **1976**; 73: 1447-51. https://doi.org/10.1073/pnas.73.5.1447
58. Liu YK, Lu QZ, Pei R, Ji HJ, Zhou GS, Zhao XL, *et al.* The effect of extracellular calcium and inorganic phosphate on the growth and osteogenic differentiation of mesenchymal stem cells in vitro: implication for bone tissue engineering. *Biomed Mater* **2009**; 4: 025004. https://doi.org/10.1088/1748-6041/4/2/025004
59. Lei Q, Chen J, Huang W, Wu D, Lin H, Lai Y. Proteomic analysis of the effect of extracellular calcium ions on human mesenchymal stem cells: implications for bone tissue engineering. *Chem Biol Interact* **2015**; 233: 139-46. https://doi.org/10.1016/j.cbi.2015.03.021
60. Abdollahi Boraei SB, Nourmohammadi J, Bakhshandeh B, Dehghan MM, Gonzalez Z, Ferrari B. The effect of protelos content on the physicochemical, mechanical and biological properties of gelatin-based scaffolds. *J Appl Biotechnol Rep* **2020**; 7: 41-7. https://doi.org/10.30491/JABR.2020.105919